International Journal of Remote Sensing
Vol. 30, No. 11, 10 June 2009, 2997–3011

Taylor & Francis
Taylor & Francis Group

Delineating compositionally different dykes in the Ulukışla basin (Central Anatolia, Turkey) using computer-enhanced multi-spectral remote sensing data

ÖZGÜR KALELIOĞLU†, KEMAL ZORLU†, MEHMET ALİ KURT†, MURAT GÜL‡ and CÜNEYT GÜLER*†

†Mersin Üniversitesi, Çiftlikköy Kampüsü, Jeoloji Mühendisliği Bölümü, 33343 Mersin, Turkey

‡Muğla Üniversitesi, Mühendislik Fakültesi, Jeoloji Mühendisliği Bölümü, 48000 Kötekli, Muğla, Turkey

In the Ulukışla basin (Central Anatolia, Turkey) several geological mapping campaigns were carried out using conventional field methods to delineate compositionally different Middle–Upper Eocene dykes. However, complete and correct mapping of these dykes was hampered by rugged terrain, lack of road access, wide spatial dyke distributions with small exposures and diverse weathering of these dykes. For these reasons, Landsat-5 Thematic Mapper (TM) satellite image of the study area was used to facilitate delineation of the exact boundaries of gabbroic, dioritic and trachytic dykes found in the area. Remotely sensed data were analysed using several image enhancement procedures, including colour composites, band ratios, principal components analysis (PCA), and Crosta technique. Results obtained from all the processes were examined, and it was found that dyke boundaries are best visible in the PCA123 image; RGB 731 colour composite; TM band ratio 5/7, 5/1, 4 combination; and 1457-PC4 image obtained by Crosta technique. The alteration differences of three dyke groups are enhanced much better in the 1457-PC4 image obtained by Crosta technique, which highlights the hydroxyl-bearing minerals as white-coloured pixels. Using computer-enhanced multi-spectral remote sensing data, we were able to map the boundaries and spatial distributions of compositionally different dykes, which otherwise is an overwhelmingly difficult task to achieve using conventional field methods. In similar settings, remote sensing techniques applied in this study may provide an efficient and low-cost alternative to time-consuming and physically demanding field-mapping campaigns.

1. Introduction

The study area (Ulukışla basin) is a highly complex and rugged mountain landscape, with elevations ranging from 900 m to 2200 m above mean sea level (amsl). In this mountainous terrain, several geological mapping campaigns were carried out using conventional field methods to delineate compositionally different dykes occurring in the area. However, complete and correct mapping of these dykes in previous studies (Alpaslan *et al.* 2003, 2004, 2006, Kurt 2004) was hampered by the roughness of the terrain, lack of road access, wide spatial distribution with small dyke exposures and diverse weathering of these dykes. Furthermore, due to three-dimensional surface

*Corresponding author. Email: cguler@mersin.edu.tr

International Journal of Remote Sensing
ISSN 0143-1161 print/ISSN 1366-5901 online
http://www.tandf.co.uk/journals
DOI: 10.1080/01431160802558683

heterogeneity of the study area, observations were rarely sufficiently dense to accurately characterize their shapes and regional distributions. This is important because these dykes may provide important clues about the tectonic regime, basin evolutionary history and the location of the areas of iron oxides and/or hydrous minerals that might be associated with the hydrothermal alteration zones of ore deposits (Tangestani and Moore 2001, Khan and Glenn 2006).

Landsat images have been used increasingly during the last two or three decades for mapping, structural analysis and economic raw material prospecting in geological studies (e.g. Khan and Glenn 2006, Khan *et al.* 2007). It is widely accepted that remotely sensed multi-spectral satellite imagery conveys useful information for mapping volcanic or similar rock types, as well as their alteration products (Abrams *et al.* 1983, Crosta and Moore 1989, Loughlin 1991, Nalbant and Alptekin 1995, Torres-Vera and Prol-Ledesma 2003, Ramadan and Kontny 2004). Landsat images also have good spectral resolution and are very useful for elucidating the different types of minerals (Ricotta *et al.* 1999). The remotely sensed response is predominantly a function of the properties of the Earth's surface. Therefore, delineating compositionally different dykes is a challenging task due to high spatial and spectral diversity of the surface materials. Classification of geological units using remote sensing data in rugged mountain environments can be complicated, since anisotropic reflectance and highly variable illumination angles due to topography can affect the signal received at the sensor (Leprieur *et al.* 1988, Franklin 1991). For that reason, topographic effects should be taken into consideration by incorporating derived image layers (e.g. band ratios) to suppress possible data-processing issues. Multivariate statistical techniques, such as principal components analysis (PCA) (Abrams *et al.* 1983, Kaufman 1988, Bennett *et al.* 1993, Rutz-Armenta and Prol-Ledesma 1998) and Crosta technique (CT) (Crosta and Moore 1989, Tangestani and Moore 2002) can also be useful, as they reduce the dimensions of the data by filtering out the redundant or noisy part through a linear transformation. The overall objective of this paper was to examine whether computer-enhanced multi-spectral remote sensing data (Landsat-5 Thematic Mapper (TM) imagery) could be used to properly discriminate and map three types of compositionally different dykes found in the Ulukışla basin, Central Anatolia, Turkey.

2. Materials and methods

2.1 *Study area*

The study area is located in the Central Anatolia region of Turkey and covers about 777 km^2 between the latitudes of 37°30′15″ and 37°38′55″ N and longitudes 34°37′26″ and 34°59′40″ E (figures 1 and 2). The area has a mountainous terrain with elevations ranging from 900 m to 2200 m amsl and includes urban centres, such as Ulukışla and Çiftehan. The specific area studied encompasses unforested heterogeneous mountainous terrain with a dry climate. The vegetation cover is typical of the dry steppes of Central Anatolia. However, patches of isolated trees are often found mainly along the watercourses.

2.2 *Geological setting*

The Ulukışla basin is one of the most important Central Anatolian basins developed on the Tauride–Anatolian Platform and Menderes–Tauride Blocks during the Late Cretaceous–Tertiary (Görür *et al.* 1984, Okay *et al.* 2001, Gürer and Aldanmaz 2002) (figure 1). Different evolutionary models have been proposed for the Ulukışla

basin, such as an island-arc basin (Oktay 1982), a back-arc basin (Görür *et al.* 1998), extensional or transtensional basin (Clark and Robertson 2002) and rifted intracontinental basin (Alpaslan *et al.* 2003, 2004, 2006), and these are currently a subject of continuing debate among researchers working in the area. The geology and stratigraphy of the Ulukışla basin was described in three major units by Alpaslan *et al.* (2003), based on previous geological studies. The study area is characterized by lithological units of a diverse nature (figure 2). These units are: (1) pre-Late Cretaceous Bolkar Carbonate Platform rocks; (2) Late Cretaceous–Eocene volcano-sedimentary deposits; and (3) post-Eocene–Recent deposits.

Pre-Late Cretaceous Bolkar Carbonate Platform rocks are composed of three major units, including: (1) Palaeozoic–Early Cretaceous limestones, dolomitic limestones and dolomites; (2) Early Palaeozoic–Early Cretaceous Niğde-Kırşehir metamorphic rocks (quartzite, gneiss, amphibolite, mica schist, marble, dolomitic marble, cherty limestone, granodiorite, monzonite and syenite); and (3) Late Cretaceous Alihoca ophiolite (serpantinized peridotite, pyroxenite, ultramafic cumulates, gabbro, microgabbro and dyke complexes) (Çevikbaş and Öztunalı 1992, Göncüoğlu *et al.* 2001).

Late Cretaceous–Eocene deposits are represented by a complex volcano-sedimentary sequence, including Late Cretaceous–Paleocene Çiftehan Formation, Paleocene–Eocene Ulukışla Formation, and Middle–Late Eocene Hasangazi Formation. The Çiftehan Formation contains agglomerate, limestone olistoliths, claret-red and grey-coloured limestones, sandstone and claystone alternations (Demirtaşlı *et al.* 1984, Çevikbaş and Öztunalı 1992, Clark and Robertson 2002, 2005). The Ulukışla Formation includes deep-sea sediments, volcano-sedimentary units and shallow-marine carbonates, all of which were cut through by Middle–Late Eocene calk-alkaline and shoshonitic dykes of dioritic, gabbroic and trachytic compositions (Çevikbaş and Öztunalı 1992, Boztuğ *et al.* 2001, Alpaslan *et al.* 2003, 2004, 2006). The Hasangazi Formation includes limestone, claystone–sandstone–conglomerate alternations (Demirtaşlı *et al.* 1984, Clark and Robertson 2005).

Post-Eocene–Recent deposits are composed mostly of continental sedimentary units and evaporites (Zeyvegediği anhydrite) (Demirtaşlı *et al.* 1984, Nazik and Gökçen 1989, Clark and Robertson 2005).

2.3 *Mineralogical and geochemical characteristics of the dykes*

Detailed mapping of the geological units in the study area was conducted by Alpaslan *et al.* (2003) and it is presented in figure 2. Nomenclature for the dykes described in this study is based on both field and geochemical classifications (Kurt 2004, Alpaslan *et al.* 2006). Mineralogical and geochemical analyses conducted in the area have revealed three compositionally different dyke units: (1) dioritic ones with 0.50–0.94 wt% TiO_2, 1.12–2.53 wt% K_2O, 2.97–6.46 wt% MgO, 52.67–57.52 wt% SiO_2 and 4.41–8.02 wt% Fe_2O_3; (2) gabbroic ones with 0.89–1.46 wt% TiO_2, 1.66–5.07 wt% K_2O, 3.05–6.49 wt% MgO, 46.86–51.98 wt% SiO_2 and 6.03–8.52 wt% Fe_2O_3; and (3) trachytic ones with 0.35–0.60 wt% TiO_2, 4.82–10.78 wt% K_2O, 0.24–1.74 wt% MgO, 59.23–63.77 wt% SiO_2 and 2.48–4.16 wt% Fe_2O_3. A more detailed discussion on the subject can be found in Alpaslan *et al.* (2006), hence, these dyke units will be described briefly here.

In the study area, dioritic dykes (named Yağlıtaş diorite) are found as elongated bodies in an east–west direction between Koçak and Ardıçlı villages (figure 2). They

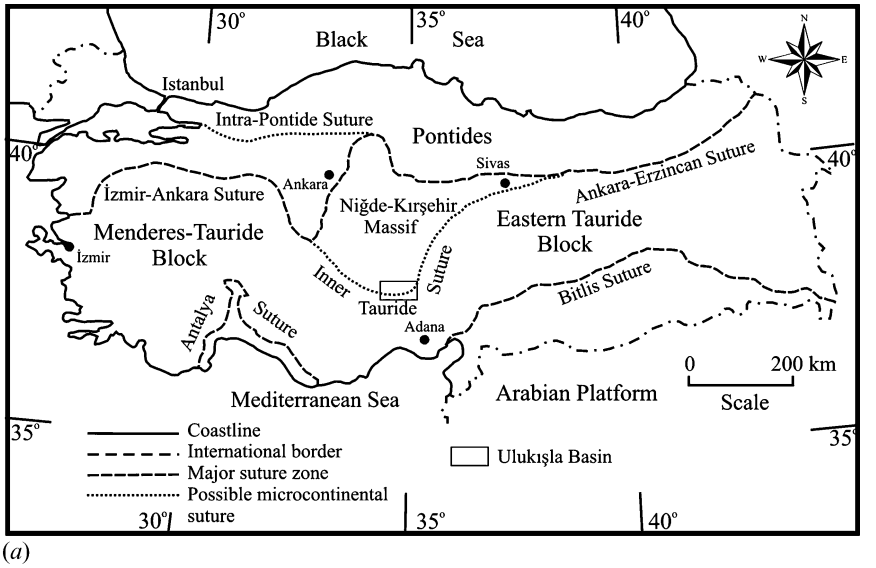

(*a*)

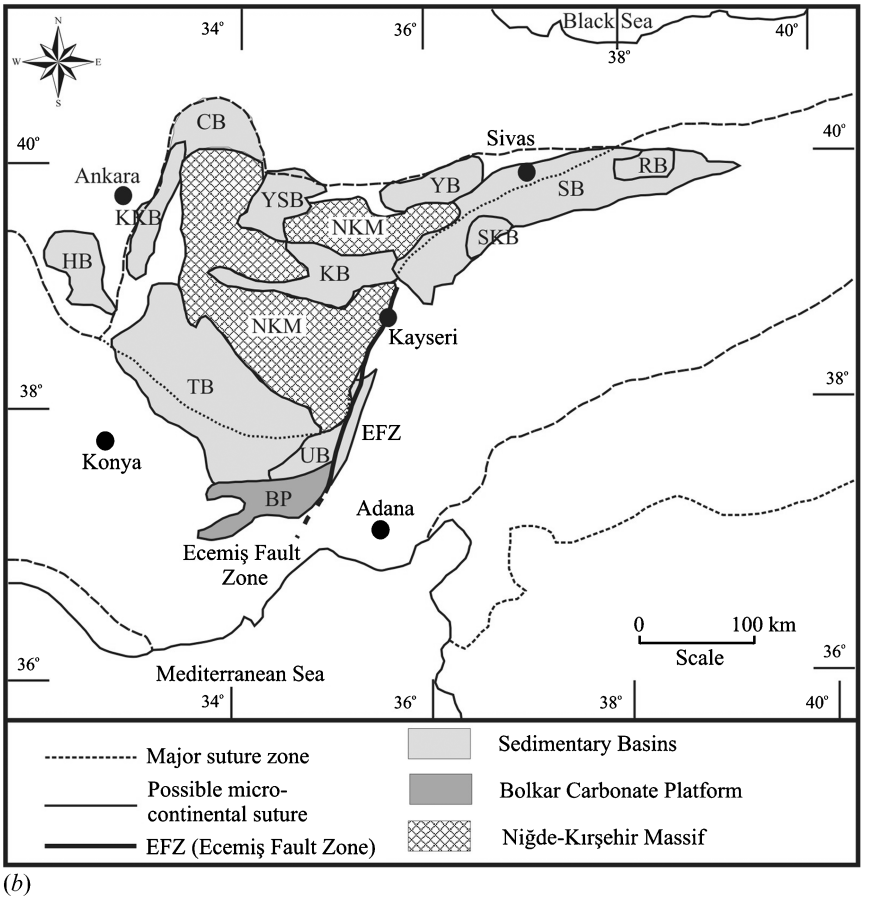

(*b*)

Figure 1. (*a*) Location of the study area and Neotethyan sutures of Turkey (after Clark and Robertson 2002). (*b*) Major sedimentary basins of Central Anatolia: Çankırı basin (CB), Haymana basin (HB), Kırıkkale basin (KKB), Kızılırmak basin (KB), Refahiye basin (RB), Şarkışla basin (SKB), Sivas basin (SB), Tuzgölü basin (TB), Ulukışla basin (UB), Yıldızeli basin (YB), Yozgat-Sorgun basin (YSB) (after Clark and Robertson 2002).

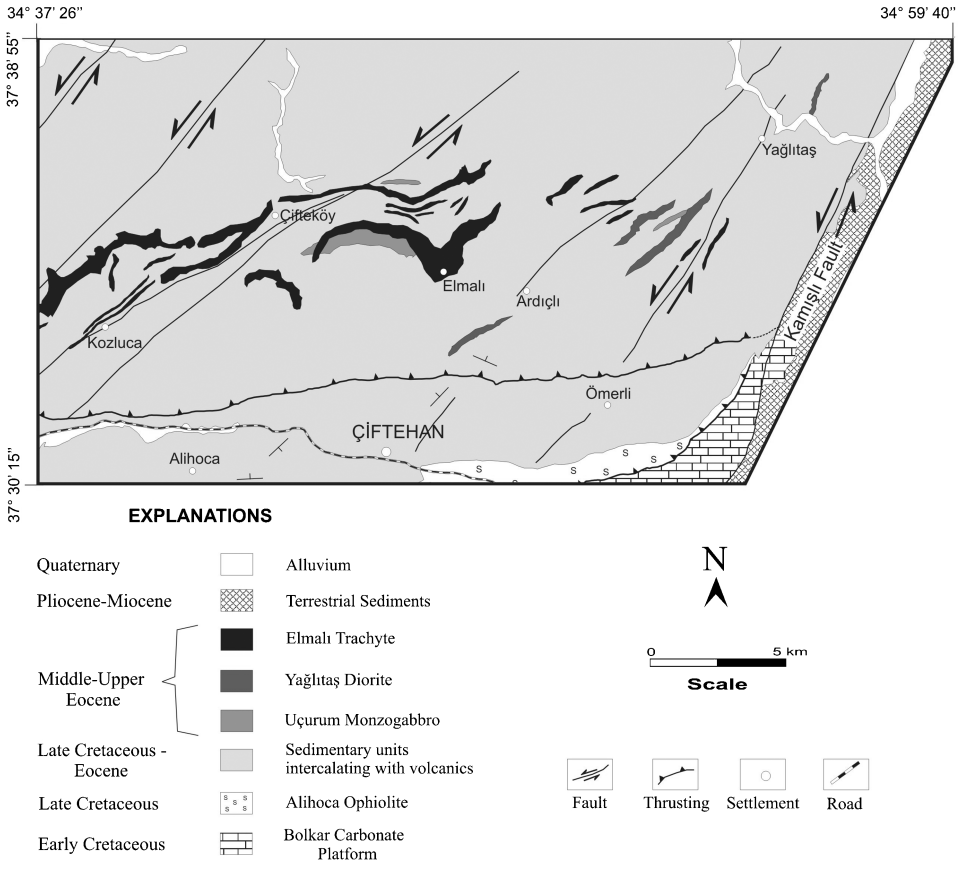

Figure 2. Geological map of the study area (modified after Alpaslan *et al.* 2003).

reach up to 7 km in length and 1 km in width. Dioritic dykes contain plagioclase, hornblende, biotite, quartz, apatite, zircon, titan and opaque minerals and are generally observed to be of light-dark grey and greenish colours in the field. When altered, they show brownish and yellowish-grey shades of colour. In the Ulukışla basin, gabbroic dykes (named Uçurum monzogabbro) are generally found around Uçurum Hill and in the east and south-east of Gedelli village (figure 2). These dykes are generally 500 m in width and their lengths can reach up to several kilometres. Gabbroic dykes include clinopyroxene, biotite, orthoclase, apatite and opaque minerals and are generally observed in the field to be of light-dark green, greyish and blackish colours. Trachytic dykes (named Elmalı trachyte) are generally elongated in the east–west direction and they are found mostly north-north-east of Ulukışla and Çiftehan towns (figure 2). These dykes are concentrated mostly in an area 15×30 km and they can reach up to 500 m in width. Trachytic dykes include sanidine, biotite, plagioclase, to a lesser extent clinopyroxene and opaque minerals and are generally observed in the field to be of brown, red or grey colours. In most places these dykes are weathered and their alteration products include chlorite, epidote, serisite, calcite and clay minerals for gabbroic dykes; chlorite, epidote and calcite for dioritic dykes; and chlorite and various clay minerals for the trachytic dykes (Kurt 2004, Alpaslan *et al.* 2003, 2004, 2006).

2.4 *Satellite data and image processing*

The multi-spectral remote sensing image used in this study consists of a cloud-free Landsat-5 TM scene (WRS-2 Path/Row: 176/34), which was acquired during the dry season on 9 June 1987. The sixth band (thermal infrared, TIR) was not used in this study due to its low spatial resolution (120 m). The Landsat-5 TM image used in this study can be viewed at the USGS Earth Resources Observation and Science (EROS) website (http://glovis.usgs.gov).

After data acquisition, several image-processing steps were completed. Initially, a subset of 1148 columns by 752 rows covering the study area was extracted from the raw Landsat-5 TM scene. The satellite data were then geometrically corrected (geo-rectified) using well-defined ground control points (GCPs; $n=30$) from the 1 : 25 000-scale topographic map sheets produced by the Turkish Ministry of Defence General Command of Mapping. First-hand knowledge of the site greatly enhanced the selection and verification of GCPs. The image was registered to real-world coordinates using the Universal Transverse Mercator (UTM) projection system with grid zone number 36S and WGS84 datum. A first-order polynomial transformation and nearest-neighbour resampling method was applied to create the output images, with 30 m ground resolution. The rms. error was less than 0.4 pixels. The Landsat-5 TM image was radiometrically corrected for enhancement of the image. Radiometric enrichment comprises the linear contrast, histogram equalization, balance contrast enhancement on the single band (Liu and Moore 1989) and band ratioing (R), principal components analysis (PCA) and Crosta technique (CT) on the multiple bands (Sabins 1987, Crosta and Moore 1989, Lillesand and Kiefer 1994). These image enhancement procedures are applied routinely to multi-spectral optical remote sensing data for easier visual analysis of the RGB (Red–Green–Blue) colour composites. No cloud correction was made since imagery was acquired under clear-sky conditions.

3. Results

In this study, a sub-scene of 176/34 (Path/Row) Landsat-5 TM multi-spectral remote sensing image was processed by several sophisticated mathematical and statistical image enhancement techniques to transform the data into meaningful map information. The image enhancement processes used in this study include colour composites (CC), TM band ratios, PCA and CT. The spectral enhancements led to multi-spectral, false-colour composites or grey-scale images which were evaluated for the discrimination of the three compositionally different dyke types (dioritic, gabbroic and trachytic) and their alteration products within the study area (figure 2). Geological maps produced during previous field investigation campaigns (Alpaslan *et al.* 2003) were used for comparison and to verify the remote sensing analyses and interpretations.

3.1 *Colour composites*

Colour composite is an image produced by displaying multiple spectral bands as colours different from the spectral range in which they were taken. This method is commonly used for displaying multi-band (multi-channel) imagery. This is usually achieved by assigning three of the image bands to the fundamental colours red (R), green (G) and blue (B), the combination of which results in a RGB (false) colour composite image. In this study, different RGB combinations were tested to see which colour composite map highlighted the differences in geology best. For example,

Aydal *et al.* (2003) preferred RGB 751 colour composite for separating the ophiolite rocks in their study. This colour composite also performed well in our study for separating the ophiolite rocks exposed in the SE of the study area, where they were shown dominantly in dark blue colours and the rest of the units in pastel tones (not shown here). However, it failed to discriminate the volcanic rock areas from ophiolite rocks due to their relatively similar spectral characteristics as a result of their alteration. Contrast enrichment for RGB 751 combination caused only expansion of intensity interval, thus the image still stayed in pastel colour tones. Through experimentation using different band combinations, it was found that lithological boundaries between the ophiolite rocks, dyke complexes and the volcano-sedimentary sequence are visible best in RGB 731 colour composite, where brownish-grey areas represent dioritic dykes, livid-coloured areas represent gabbroic dykes and yellowish-greenish-brown areas represent trachytic dykes (figure 3(*a*)). Although, colour composite maps provided a relatively easy and fast method to display the multi-spectral information, they do not provide a detailed map for the separation of the individual units or the alteration zones. Thus, additional image enhancement processes are required for their separation.

3.2 *Band ratioing*

Another useful approach for separating different lithological units is the application of band ratios to the Landsat TM bands (band ratioing). This technique was applied successfully in several studies dealing with lithology discrimination and hydrothermal alteration mapping (Hunt *et al.* 1973, Hunt and Ashley 1979, Hunt 1980, 1981). Spectral characteristics of the minerals are used to decide the pairs of bands to be ratioed. Band ratio technique is based on highlighting the spectral differences unique to the materials being mapped. The band ratioing technique used in this study follows the general methodology of Ramadan and Kontny (2004), who noted that certain band ratios of Landsat TM are particularly useful for lithological discrimination. Ramadan and Kontny (2004) used TM band ratio 5/7, 5/1, 4 combinations for discriminating the compositionally different volcanic and ophiolitic rocks. In their study, volcanic rocks appeared in dark green colours, felsic volcanic rocks appeared in light green colours and ultramafic rocks appeared in red colours. A similar colour composition was also observed in the Ulukışla basin using the same band ratio combination. In our study, using TM band 5/7, 5/1, 4 ratio image, the trachytic dykes are shown in pinkish-green colours, gabbroic dykes in bluish-pale green colours, and dioritic dykes in brownish-dark green colours. Ophiolitic rocks in the SE of the region were represented by dark red, claret-red colours (figure 3(*b*)). It is generally accepted that clay minerals exhibit strong absorption in TM band 7 (2080–2350 nm) and high reflectance in TM band 5 (1550–1750 nm) (Aydal *et al.* 2007). For that reason, band ratioing these bands (TM band 5/7) has the potential to enhance the clay minerals in the final image.

3.3 *Principal Components Analysis (PCA)*

As discussed earlier, the spectral information of different bands is often strongly correlated. As indicated by the correlation coefficients (table 1), very high correlations exist within the visible (450–690 nm) and infrared (750–2350 nm) spectra and, therefore, their information is redundant. However, low correlation coefficients exist between the TM band 1–4, 2–4, 3–4, 5–4 and 7–4 pairs, where TM

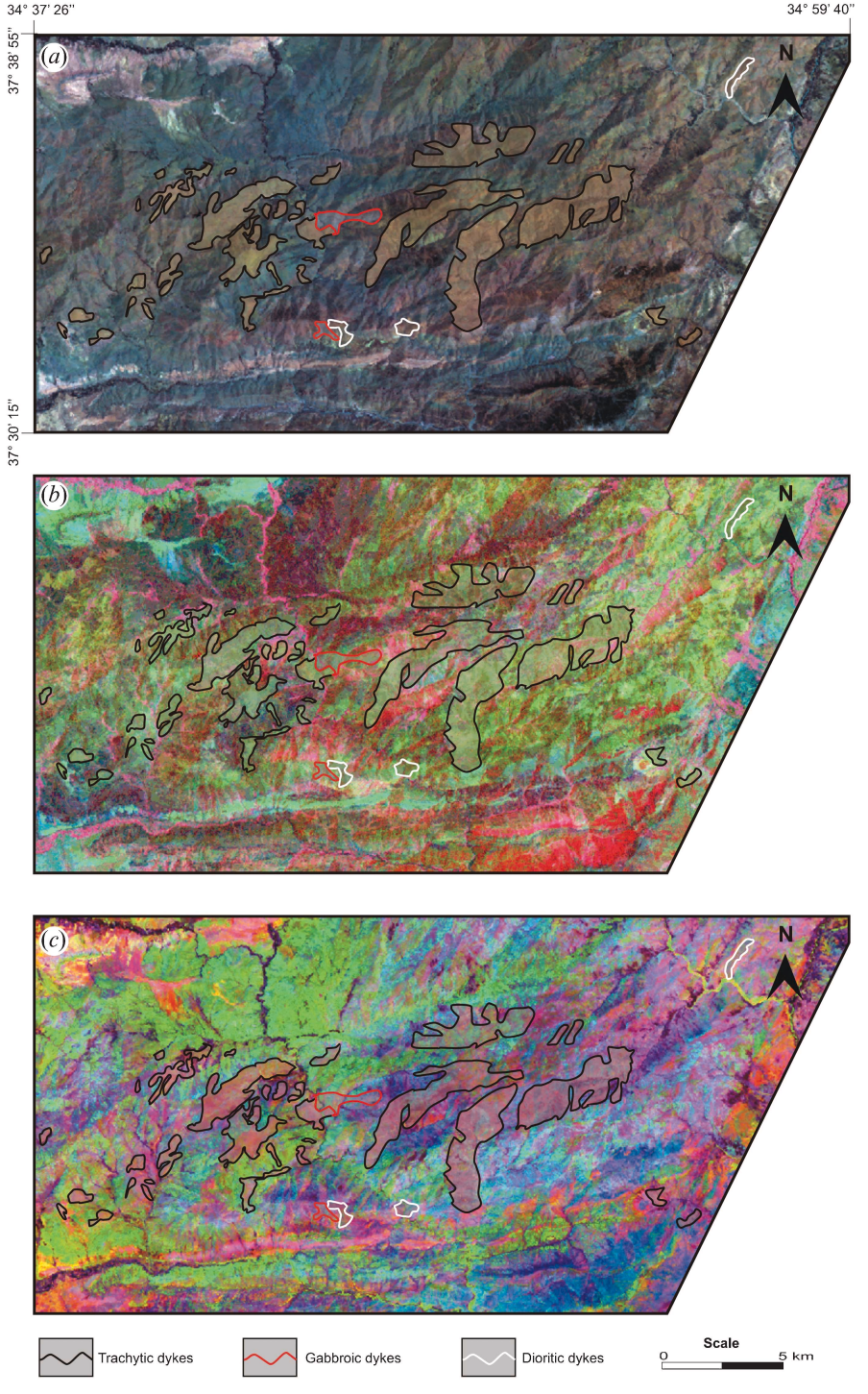

Figure 3. (*a*) Colour composite Landsat TM 731 displayed in RGB space. (*b*) Colour composite of the Landsat TM band ratios 5/7, 5/1, 4 displayed in RGB space. (*c*) Colour composite PC123 image obtained after PCA applied to the selected six TM bands (1–5 and 7). For interpretation of the references to colours in this figure, the reader is referred to the web version of the article.

Table 1. Correlation matrix of the non-thermal TM bands (1–5 and 7).

TM bands	1	2	3	4	5	7
1	1.000					
2	0.955	1.000				
3	0.926	0.976	1.000			
4	0.374	0.494	0.430	1.000		
5	0.704	0.821	0.813	0.613	1.000	
7	0.795	0.883	0.893	0.483	0.961	1.000

band 4 shows the lowest correlations of all the non-thermal TM bands. Judging by this result, a combination of TM bands 1, 4, 5 and 7 would represent the most uncorrelated bands. Hence, colour composite maps produced using these bands have the potential to discriminate compositionally different dykes occurring in the study area.

Intrusive dyke rocks of the Ulukışla basin show various alteration products, including chloritization, biotitization, sericitization, epidotization, carbonation and silicification. To highlight these alteration zones, PCA was conducted on the selected six non-thermal bands of the Landsat TM image and results are shown in table 2. Eigenvalues and eigenvector values for the PCA transformation give some interesting information. PCA analysis results show that the first three PCs (PC1, PC2 and PC3) explain almost all the variance contained in the multi-spectral data, which is indicated by their high eigenvalue percentages. PC1 basically gives information about the albedo and topography, which is indicated by its high eigenvalue (table 2). Incorporating PC1 in the RGB colour composites better highlights the topographic effects and provides an easier visual interpretation. PC2 is related mainly to vegetation, because TM band 4 has high negative loading (−0.85) in this component. In PC3, there is no dominant band and almost all the bands show similar values but reverse signs. TM bands 1 and 3 mostly contribute to PC4, with values 0.70 and −0.64, respectively. PC5 highlights mostly the hydroxyl-bearing minerals. TM band 5 has a negative loading (−0.39), whereas TM band 7 shows a high loading value with positive sign (+0.83). The most prominent band in PC6 is TM band 2, which is indicated by its high loading value (0.91). The PC combination PC123 was chosen because PC1 gives information mostly about albedo and topographic effects (dykes mostly occur in topographically high areas), PC2 was preferred due to high loadings in TM band 4, which gives information about the vegetative colour differences, and PC3 basically gives information about hydroxyl-

Table 2. Eigenvector matrix and eigenvalues obtained by principal components analysis (PCA) on six TM bands (1–5 and 7).

	TM bands						Eigenvalue
Principal component	1	2	3	4	5	7	(%)
PC1	0.25	0.20	0.34	0.26	0.73	0.43	83.55
PC2	0.31	0.15	0.33	−0.85	−0.12	0.20	10.02
PC3	−0.52	−0.29	−0.43	−0.43	0.51	0.17	5.46
PC4	0.70	0.02	−0.64	−0.07	0.21	−0.22	0.58
PC5	0.11	−0.14	−0.32	0.14	−0.39	0.83	0.33
PC6	−0.27	0.91	−0.29	−0.03	−0.05	0.06	0.07

bearing minerals because of high loadings of TM bands 1 and 5, respectively (table 2). Information from six TM bands is transformed using PCA to three processed images (PC1, PC2 and PC3) that contain virtually all of the variance. The three output bands were displayed simultaneously as components of an RGB display. In the colour composite map produced using PC123, greenish-purple areas indicate the dioritic dykes, bluish-purple areas the gabbroic dykes and greenish-yellowish purple areas the trachytic dykes (figure 3(*c*)).

3.4 *Crosta technique*

In this technique, target components (materials of interest) are represented by bright or dark-coloured pixels based on signs and magnitudes of the eigenvector loadings (Loughlin 1991). This technique is generally applied to four and six selected bands of TM data to detect anomalous concentrations of hydroxyl, hydroxyl plus iron oxide and iron oxide minerals (Crosta and Moore 1989, Rutz-Armenta and Prol-Ledesma 1998, Ranjbar *et al.* 2004). The transformation of the PCs on TM bands 1, 4, 5 and 7 of the Ulukışla basin sub-scene is given in table 3. In this PCA analysis, TM bands 2 and 3 were omitted on purpose in order to suppress iron oxide. This analysis also forms the basis for the commonly used Crosta technique. This method was followed for hydroxyl mapping and employs only four TM bands during PCA and includes the analysis of the eigenvector loadings for TM bands 5 and 7. Four band PCA analysis results show that the first two or three PCs (PC1, PC2 and PC3) explain almost all the variance contained in the multi-spectral data, which is indicated by their high eigenvalue percentages. Even though, PC4 has the lowest eigenvector value, it contains important information about hydroxyl-bearing minerals (alteration products), which is indicated by medium to high loadings of TM bands 5 and 7 (-0.45 and $+0.84$, respectively) on PC4. Therefore, single band (grey-scale) 1457-PC4 image (the fourth PC image of the PCA on TM bands 1, 4, 5, 7) highlights the hydroxyl-bearing minerals as white pixels in figure 4. White areas in this figure also correspond well to weathered areas (volcanic rocks), indicated in previous field-based studies. However, it should be noted that white pixels in 1457-PC4 image also partly represent the alluvial deposits and weathered areas of ophiolitic rocks.

4. Discussion

Landsat TM multi-spectral remote sensing imagery provides a potentially useful data source that can be used for classification of geological units as well as their alteration products, especially in remote and rugged mountainous areas, such as the Ulukışla basin (Central Anatolia, Turkey). In Ulukışla basin, several geological

Table 3. Eigenvector matrix and eigenvalues obtained by principal components analysis (PCA) on four TM bands (1, 4, 5 and 7).

Principal component	TM bands				Eigenvalue (%)
	1	4	5	7	
PC1	0.25	0.29	0.80	0.46	84.76
PC2	−0.24	0.92	−0.09	−0.29	10.68
PC3	−0.90	−0.21	0.39	−0.05	4.10
PC4	−0.28	0.15	−0.45	0.84	0.46

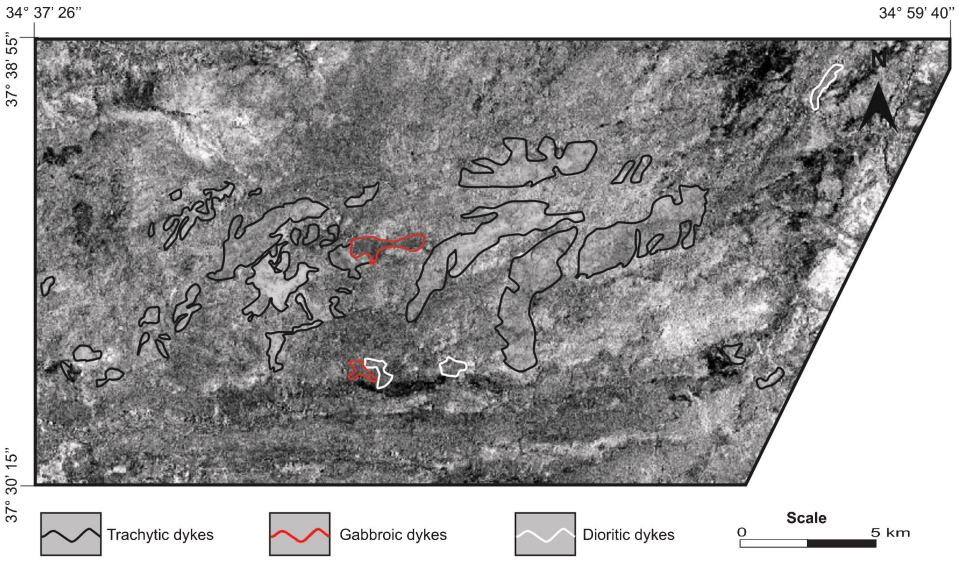

Figure 4. Grey-scale 1457-PC4 image obtained after PCA applied to four selected TM bands (1, 4, 5 and 7). Bright pixel areas indicate the alteration products (hydroxyl-bearing phases). For interpretation of the references to colours in this figure, the reader is referred to the web version of the article.

mapping campaigns were carried out using conventional field-based methods to delineate three types of compositionally different dykes (dioritic, gabbroic and trachytic in composition) occurring in the area. Unfortunately, several compounding factors (roughness of the terrain, lack of road network, irregular dyke distributions with small exposures and diverse weathering of these dykes) prevented accurate and complete mapping of them (Kurt 2004, Alpaslan *et al.* 2003, 2004, 2006). Discrimination and correct mapping of these dykes are important because they provide important clues about the tectonic regime, basin evolutionary history and the location of the areas of iron oxides and/or hydrous minerals that might be associated with hydrothermal alteration zones of ore deposits (Tangestani and Moore 2001, Khan and Glenn 2006).

The methodology included the selection of combinations of data channels and their transformations to enhance the discriminative power of the lithology classification. In addition to the ordinary RGB colour compositing (e.g. RGB 731 image), supplementary image processing techniques, such as band ratioing (TM band ratio image 5/7, 5/1, 4) and principal component analysis (PCA123 image), were used to discriminate and map these dykes based on mineralogical composition of geological units and their alteration products. The resultant images from the analysis of the Landsat dataset included larger dyke areas than the previous field-based studies. Also, compared to geological maps, we found that the image of 1457-PC4 obtained by Crosta technique approximately predicted the altered rocks in study area. Given the results of Landsat TM image classifications obtained in this study, derived maps appear to discriminate fairly accurately the three types of compositionally different dykes occurring in the Ulukışla basin (table 4). The overall classification accuracy for different methods ranges between 69.8% and 92.7%. The highest overall accuracy was achieved by the PCA123 image (92.7%). For the other methods (RGB 731 colour composite, TM band ratio 5/7, 5/1, 4 combination and

Table 4. Properties of the maps produced by different image-enhancement techniques used in this study.

Method	TM bands used	Band assignment (R: red; G: green; B: blue)	Details	Overall accuracy (%)
Colour composite (CC)	1, 3, 7	R=7; G=3; B=1	Compositionally different dykes well separated	83.3
Band ratioing (R)	1, 4, 5, 7	R=5/7; G=5/1; B=4	Compositionally different dykes well separated	81.2
PC analysis (PCA)	1, 2, 3, 4, 5, 7	R=PC1; G=PC2; B=PC3	Compositionally different dykes well separated	92.7
Crosta technique (CT)	1, 4, 5, 7	Grey-scale= 1457-PC4	Shows alteration (hydroxyl-bearing) products	69.8

1457-PC4 image obtained by Crosta technique), the overall classification accuracy was 9.4–22.9% lower than the PCA method (table 4).

Dykes of the Ulukışla basin show various types and variable degrees of alteration in the field. Therefore, irregular distribution of the alteration products causes different reflectance values in TM band records. Thus, in the colour composite images produced using various sophisticated techniques, a homogeneous colour distribution cannot be observed. Successive RGB colour composites produced by different techniques (e.g. RGB colour composite, band ratioing and PCA) may help to clarify some ambiguities, improve the hue, intensity and contrast, and provide easier visual image interpretation. The methods and parameters used in image enhancement processes and employed during this study are summarized in table 4.

5. Conclusions

In general, the maps derived from remote sensing data agree well with the field-derived maps and show details unobtainable from conventional ground-based mapping (see section 4). Results obtained from all the methods were examined, and it was found that dyke boundaries are visible best in the PCA123 image; RGB 731 colour composite; TM band ratio 5/7, 5/1, 4 combination; and 1457-PC4 image obtained by Crosta technique. The alteration differences of three dyke groups are enhanced much better in the 1457-PC4 image obtained by Crosta technique, which highlights the hydroxyl-bearing minerals as white pixels. However, computer-enhanced image classification is not considered here as a technique aimed at completely replacing traditional geological mapping. Instead, it is conceived as a technique to assist the geologist in map compilation and the identification of areas for map refinement. Despite good predictive abilities obtained in this study, approaches for discriminating compositionally different dykes must be assessed further before they can be considered reliable and robust predictive tools. Thus, the further testing of these techniques over larger geographical extents is required. While we have limited our study to multi-spectral remote sensing in the visible and near-infrared, mid-infrared and shortwave infrared optical domain, remote sensors operating in other regions of the electromagnetic spectrum (e.g. TIR, microwave and hyperspectral remote sensing) can also be useful for this particular application. Future studies should explore these technologies further.

Acknowledgements

The authors would like to express their gratitude to Prof. Musa Alpaslan for providing the geochemical data on the dykes of the Ulukışla basin and for sharing the field information to support the research.

References

ABRAMS, M.J., BROWN, L., LEPLEY, R. and SADOWSKI, P., 1983, Remote sensing for porphyry copper deposits in southern Arizona. *Economic Geology*, **78**, pp. 591–604.

ALPASLAN, M., BOZTUĞ, D., FREI, R., TEMEL, A. and KURT, M.A., 2006, Geochemical and Pb–Sr–Nd isotopic composition of the ultrapotassic volcanic rocks from the extension-related Çamardı–Ulukışla basin, Niğde Province, Central Anatolia, Turkey. *Journal of Asian Earth Sciences*, **27**, pp. 613–627.

ALPASLAN, M., BOZTUĞ, D., UÇURUM, A. and ÖZDEMIR Z., 2003, Petrology of the Palaeocene–Eocene volcanics and the gold potential of the hydrothermal occurrences in the Çamardı-Ulukışla Region (in Turkish). TÜBİTAK Project Report (unpublished) No: YDABÇAG-100Y010.

ALPASLAN, M., FREI, R., BOZTUĞ, D., KURT, M.A. and TEMEL, A., 2004, Geochemical and Pb–Sr–Nd isotopic constrains indicating and enriched-mantle sources for Late Cretaceous to Early Tertiary volcanism, Central Anatolia, Turkey. *International Geology Review*, **46**, pp. 1022–1041.

AYDAL, D., ALTAŞ, M. and POLAT, O., 2003, Usage of Geographic Information Systems with the remote sensing techniques for geological mapping and the ore research in the Kızıldağ ophiolites. In *Proceedings of the 10th Anniversary Symposium of the Mersin University, Department of Geological Engineering* (in Turkish), (Mersin, Turkey: Mersin University), p. 112.

AYDAL, D., ARDA, E. and DUMANLILAR, Ö., 2007, Application of the Crosta technique for alteration mapping of granitoidic rocks using ETM+ data: case study from eastern Tauride belt (SE Turkey). *International Journal of Remote Sensing*, **28**, pp. 3895–3913.

BENNETT, S.A., ATKINSON, W.W. and KRUSE, F.A., 1993, Use of Thematic Mapper imagery to identify mineralization in the Santa Teresa district, Sonara, Mexico. *International Geology Review*, **35**, pp. 1009–1029.

BOZTUĞ, D., ÇEVIKBAŞ A., DEMIRKOL, C. and ÖZTUNALI Ö., 2001, The co-existence of the crustal thickening and thinning related plutons in the Middle Taurus Mountains, Turkey. In *Proceedings of Fourth International Turkish Geology Symposium, Çukurova University*, Adana, (Adana, Turkey: Cukurova University), p. 207.

ÇEVIKBAŞ A. and ÖZTUNALI Ö., 1992, Depositional basin history of the Ulukışla-Çamardı (Niğde) after the Maastrichtian. *Bulletin of Mineral Research and Exploration Institute* (in Turkish with English abstract), **114**, pp. 155–172.

CLARK, M. and ROBERTSON, A.H.F., 2002, The role of the Early Tertiary Ulukışla basin, Southern Turkey, in suturing of the Mesozoic Tethys Ocean. *Journal of the Geological Society, London*, **159**, pp. 673–690.

CLARK, M. and ROBERTSON, A.H.F., 2005, Uppermost Cretaceous–Lower Tertiary Ulukışla Basin, south-central Turkey: sedimentary evolution of part of a unified basin complex within an evolving Neotethyan suture zone. *Sedimentary Geology*, **173**, pp. 15–51.

CROSTA, A. and MOORE, J.MCM., 1989, Enhancement of Landsat Thematic Mapper imagery for residual soil mapping in SW Minais Gerais State, Brazil: a prospecting case history in Greenstone belt terrain. In *Proceedings of the Seventh ERIM Thematic Conference: Remote Sensing for Exploration Geology*, (Calgary, AB: ERIM), pp. 1173–1187.

DEMIRTAŞLI, E., TURHAN, N., BILGIN, A.Z. and SELIM, M., 1984, Geology of the Bolkar Mountains. In *Proceedings of the International Symposium on the Geology of the Taurus Belt*, Ankara, Turkey O. Tekeli and M.C. Göncüoğlu (Eds), (Ankara, Turkey: Maden Tetkik ve Arama Enstitusu), pp. 125–141.

FRANKLIN, S.E., 1991, Image transformation in mountainous terrain and the relationship to surface patterns. *Computers and Geosciences*, **17**, pp. 1137–1149.

GÖNCÜOĞLU, M.C., TEKIN, U.K. and TURHAN, N., 2001, Geologic meaning of Late Carnien aged radiolarite bearing basalt blocks in the Late Cretaceous middle Sakarya ophiolite complex (NW Anatolia). In *Proceedings of the Congress of Geological Chamber of Turkey* (in Turkish with English abstract), (Ankara, Turkey: Geological Chamber of Turkey), pp. 54–56.

GÖRÜR, N., OKTAY, F.Y., SEYMEN, I. and ŞENGÖR A.M.C., 1984, Paleotectonic evolution of the Tuzgölü basin complex, Central Turkey: sedimentary record of a Neotethyan Closure. In *The Geological Evolution of the Eastern Mediterranean*, J.E. Dixon and A.F.H. Robertson (Eds), pp. 467–482 (London: Geological Society, London, Special Publications 17).

GÖRÜR, N., TÜYSÜZ, O. and ŞENGÖR A.M.C., 1998, Tectonic evolution of the Central Anatolian basins. *International Geology Review*, **40**, pp. 831–850.

GÜRER, Ö.F. and ALDANMAZ, E., 2002, Origin of the Upper Cretaceous-Tertiary Sedimentary Basins within the Tauride-Anatolide Platform in Turkey. *Geological Magazine*, **139**, pp. 191–197.

HUNT, G.R., 1980, Electromagnetic radiation: the communication link in remote sensing. In *Remote Sensing in Geology*, B.S. Siegal and A.R. Gillespie (Eds), pp. 5–45 (New York: Wiley).

HUNT, G.R., 1981, Spectra of kaolin minerals in altered volcanic rocks. *Clays and Clay Minerals*, **29**, pp. 76–81.

HUNT, G.R. and ASHLEY, R.P., 1979, Spectra of altered rocks in the visible and near infrared. *Economic Geology*, **74**, pp. 1613–1629.

HUNT, G.R., SALISBURY, J.W. and LENHOFF, C.J., 1973, Visible and near-infrared spectra of minerals and rocks IV. Additional silicates. *Modern Geology*, **4**, pp. 85–106.

KAUFMAN, H., 1988, Mineral exploration along the Agaba-Levant structure by use of TM-data concepts, processing and results. *International Journal of Remote Sensing*, **9**, pp. 1630–1658.

KHAN, S.D. and GLENN, N.F., 2006, New strike-slip faults and litho-units mapped in Chitral (N. Pakistan) using field and ASTER data yield regionally significant results. *International Journal of Remote Sensing*, **27**, pp. 4495–4512.

KHAN, T., MURATA, M., KARIM, T., ZAFAR, M., OZAWA, H. and REHMAN, H., 2007, A Cretaceous dike swarm provides evidence of a spreading axis in the back-arc basin of the Kohistan paleo-island arc, northwestern Himalaya, Pakistan. *Journal of Asian Earth Sciences*, **29**, pp. 350–360.

KURT, M.A., 2004, Mineralogic, petrographic and geochemical investigations of the gabbroic and dioritic dykes that cuts the Ulukışla (Niğde) volcano-sedimentary sequence. MSc dissertation, Mersin University, Mersin, Turkey.

LEPRIEUR, C.E., DURAND, J.M. and PEYRON, J.L., 1988, Influence of topography on forest reflectance using Landsat Thematic Mapper and Digital Terrain Data. *Photogrammetric Engineering and Remote Sensing*, **54**, pp. 491–496.

LILLESAND, T.M. and KIEFER, R.W., 1994, *Remote Sensing and Image Interpretation*, (New York: John Wiley & Sons, Inc.).

LIU, J.G. and MOORE, J.McM., 1989, Colour enhancement and shadow suppression techniques for TM images. In *Proceedings of the 7th (ERIM) Thematic Conference: Remote Sensing for Exploration Geology*, Calgary, Alberta, Canada, (Calgary, AB: ERIM), pp. 901–915.

LOUGHLIN, W.P., 1991, Principal component analysis for alteration mapping. *Photogrammetric Engineering and Remote Sensing*, **57**, pp. 1163–1169.

NALBANT, S.S. and ALPTEKIN, Ö., 1995, The use of Landsat Thematic Mapper imagery for analysing lithology and structure of Korucu-Duğla area in Western Turkey. *International Journal of Remote Sensing*, **16**, pp. 2357–2374.

NAZIK, A. and GÖKÇEN, N., 1989, Stratigraphical interpretations of the Ulukışla Tertiary Sequence based on foraminifera and ostracoda faunas. *Geological Bulletin of Turkey* (in Turkish with English abstract), **32**, pp. 89–99.

OKAY, A.I., TANSEL, İ. and TÜYSÜZ, O., 2001, Obduction, subduction and collision as reflected in the Upper Cretaceous–Lower Eocene sedimentary record of western Turkey. *Geological Magazine*, **138**, pp. 117–142.

OKTAY, F.Y., 1982, Stratigraphy and geological evolution of the Ulukışla and surrounding area. *Geological Bulletin of Turkey* (in Turkish with English abstract), **25**, pp. 15–23.

RAMADAN, T. and KONTNY, A., 2004, Mineralogical and structural characterization of alteration zones detected by orbital remote sensing at Shalatin District area, SE Desert, Egypt. *Journal of African Earth Sciences*, **40**, pp. 89–99.

RANJBAR, H., HONARMAND, H.M. and MOEZIFAR, Z., 2004, Application of the Crosta technique for porphyry copper alteration mapping, using ETM data in the southern part of the Iranian volcanic sedimentary belt. *Journal of Asian Earth Sciences*, **24**, pp. 237–243.

RICOTTA, C., AVENA, G.C. and VOLPE, F., 1999, The influence of principal component analysis on the spatial structure of a multispectral dataset. *International Journal of Remote Sensing*, **20**, pp. 3367–3376.

RUTZ-ARMENTA, J.R. and PROL-LEDESMA, R.M., 1998, Techniques for enhancing the spectral response of hydrothermal alteration minerals in Thematic Mapper images of Central Mexico. *International Journal of Remote Sensing*, **19**, pp. 1981–2000.

SABINS, F.F. JR., 1987, *Remote Sensing Principles and Interpretation*, (New York: W.H. Freeman and Company).

TANGESTANI, M.H. and MOORE, F., 2001, Comparison of three principal component analysis techniques to porphyry copper alteration mapping: a case study, Meiduk area, Kerman, Iran. *Canadian Journal of Remote Sensing*, **27**, pp. 176–181.

TANGESTANI, M.H. and MOORE, F., 2002, Porphyry copper alteration mapping in the Meiduk area, Iran. *International Journal of Remote Sensing*, **23**, pp. 4815–4825.

TORRES-VERA, M.A. and PROL-LEDESMA, R.M., 2003, Spectral enhancement of selected pixels in Thematic Mapper images of the Guanajuato district (Mexico) to identify hydrothermally altered rocks. *International Journal of Remote Sensing*, **24**, pp. 4357–4373.